ES Materials and Manufacturing
DOI: https://dx.doi.org/10.30919/esmm5f778

Self-assembly Study of Complex Topological Structure Constructing From Telechelic Polymer Systems

Hui Li,[1, 2,*] Zhenyu Wang,[1] Yuanyuan Wei,[1] Ning Wang,[1] Kaiming Gao,[1] Xunhua Liao,[1] Haitao Zhao,[1] Long Zhang,[1, 2] Zhenbin Chen,[1, 2] Qiaoli Lin,[1, 2] Dongdong Hu,[3,*] Juan M Ruso[4] and Zhen Liu[5,*]

Abstract

This study investigated the self-assembly behavior of active telechelic polymers with complex topological structure bydissipative particle dynamics method. Complex topologies include structures with end groups, such as"line", "star" and "tadpole", and structures without end groups, such as"ring", "flower" and "cage". The self-assembly structure distributions of polymers with complex topological structure in different solvent conditions were analyzed. These complex topologies are formed through cross-linking reactions between end groups of active telechelic polymers. The simulation results shown that the topological polymers could self-assemble to form micellar structure such as hollow vesicles, spherical, lamellar, and tubular micelles in dilute solutions. Topological polymers without end groups were more likely to form dense spherical micelles, ellipsoid micelles and vesicle. The "core" formed by the active end groups of telechelic polymers was embedded on the surface and inside of the micelles. The statistical results could reveal the conditions and self-assembly mechanism of self-assembled micelle structure of various topological polymers. The results of computer simulation research can open up research ideas in experimental scientific design and preparation of complex topological polymers. The results can provide theoretical support for obtaining thermodynamically stable self-assembled structure and support the development of new materials.

Keywords: Polymer; Structure; Topological; Self-assembly.
Received: 22 June 2022; Revised: 11 August 2022; Accepted: 23 September 2022.
Article type: Research article.

1. Introduction

Topological structure is the mainintrinsic factor determining the properties of polymers materials.[1] In order to obtain accurate advanced materials with long range order, researchers can change the topological structure of polymers from the research source to achieve the regulation of advanced self-assembled structure. At present, more and more researchers are designing and synthesizing topological polymers with novel structure to obtain polymer materials with unique properties.[2-4] These polymer materials have regular self-assembly structures. Previous studies have found that the same composition of polymers with different topological morphology could form complex micelles under the same conditions.[5] These micelles show great differences in particle size, morphology, temperature and other environmental sensitivity.

Telechelic polymers are a special form of line hetero polymers that generally have the same end group at both ends.[6] Such polymers with bi-functional end groups can be synthesized experimentally by free radical initiators or chain transfer agent with specific functional groups. Since the active end groups of telechelic polymers can further react, telechelic polymers are usually used as cross-linking agent, chain extender or macromolecule. Which can build polymers with complex topological structure such as block copolymers, graft copolymers, hyperbranched polymers and dendrimers, *etc*. Therefore, significant economic and research value belong to

[1] *School of Material Science and Engineering, Lanzhou University of Technology, Lanzhou, 730050, Gansu, China.*
[2] *State Key Laboratory of Advanced Processing and Recycling of Non-ferrous Metal, Lanzhou University of Technology, No. 287 Langongping Road, Lanzhou, 730050, Gansu, China.*
[3] *State Key Laboratory of Chemical Engineering, East China University of Science and Technology, Shanghai, 200237, China.*
[4] *Soft Matter and Molecular Biophysics Group, Department of Applied Physics, University of Santiago de Compostela, 15782 Santiago de Compostela, Spain.*
[5] *Department of Physics and Engineering, Frostburg State University, Frostburg, MD, 21532, USA.*
[*] *Email:* lihui0226@163.com (H Li); hudd@ecust.edu.cn (D Hu); zliu@frostburg.edu (Z Liu).

this active telechelic polymer.[7-14] At present, telechelic polymers have been widely used in biomedicine, optical research, chemical production and other fields.[15-18] As a new carrier of water-soluble drugs, amphiphilic Lipid-PEG can self-assemble into nearly spherical micelles in aqueous solution, which can well control the release of hydrophobic drugs. The functional pattern surfaces, obtained from surface pretreated and solution impregnated end-anchored fluorescent-labeled polymethyl methacrylate (PMMA) ultrathin films can be applied to sensing, light harvesting, or organic electronics. Studies in the production and prepolymer of lactyl-lactic acid found that carboxyl terminal bonding can improve the thermal stability of polylactic acid polymer. Hydroxyl terminal bonding can improve the production speed and efficiency of lactyl-lactic acid.

With the advancement of synthesis technology, a variety of polymers with complex topological structures can be synthesized by using telechelic polymers as intermediates. These complex topological polymers can be further self-assembled to form rich and ordered nanostructure. A series of research results show that the alkynyl-terminated telechelic polyimide can effectively enhance the mechanical properties of carbon fiber cloth.[19] The water resistance and mechanical properties of the waterborne polyurethane-polymethyl methacrylate film prepared by the reversible addition chain transfer radical polymerization method have been obviously improved.[20] A series of carboxyl-terminated telechelic polyolefin prepolymers with high heat resistance can be synthesized by ring-opening metathesis copolymerization.[21] Therefore, clarifying the mechanism of complex topological structure and its self-assembly structure based on telechelic polymer can provide a bottom-up analysis for the development of materials with ideal properties. Furthermore, polymers can be adjusted to obtain ideal materials through controlling the topological structure of amphiphilic polymers.

In order to study the effect of topological structure on self-assembly behavior of polymers, it is necessary to clearly understand the self-assembly dynamic mechanism of polymers with various topological structures.[22,23] Due to the fast process it is difficult to observe the polymer self-assembly in detail at microscopic and mesoscopic scales in experimental studies.[24] For this reason, computer simulation shows innate superiority. Computer simulation can effectively make up for the experimental research constraints of micro/mesoscopic scale dynamic self-assembly behavior of the polymer structure.[25,26] By designing chemical or topological different molecular structure, various stability state of multistage self-assembled aggregation structure can be predicted and applied to further predict their physical and chemical properties.[27] As the finding by Ma *et al.*,[28] the degree of stretching of polymer chain gradually grown with the increase of $\alpha(A,B)$in spherical micelles and vesicles. The degree of stretching of hydrophobic segment (B) decreased when the morphologies changed from sphere to disk-like micelle. The results of computer simulation can not only be used as a theoretical guide to explain the experimental results,[29] but also predict the form of macromolecule self-assembly aggregates from the molecular structure, providing design schemes for screening new materials.[30] Moreover, the vesicles formed by composite materials can better meet the actual demand, and show the potential for application in the fields of drug therapy and cosmetics due to the designability of composite materials.[31-33]

In this paper, dissipative particle dynamics (DPD) method was employed to study the self-assembly behavior of various complex topological polymers based on active telechelic polymers. Complex topological structure such as “line”, “star”, “tadpole”, “ring”, “cage” and “flower” were formed by cross linking reaction between active end groups. We further counted the micelle structure formed by self-assembly of polymers with various topological structure, and explained the formation mechanism of micelle structure. Through the detailed statistics of the self-assembled micelle structure of polymers with various topological structure, we analyzed the formation conditions of micelle structure and clarified the formation mechanism of micelle structure.

2. Method and model

Dissipative particle dynamics (DPD) method is a coarse-grained simulation method at mesoscopic scale, which was invented and developed by Hoogerbrugge and Koelman in 1992 and successfully applied by Groot and Warren in 1997.[34,35] In DPD, each particle (usually called a bead) represents the entire molecular fragment or fluid element. This feature allows DPD method to use a large integral time step and conduct time dynamics simulation at mesoscopic scale.[36]

2.1 Simulation method

DPD method is a mathematical calculation method based on the classical Newton equation of motion.[37]

$$\frac{\mathrm{dr_i}}{\mathrm{dt}} = \mathrm{v_i},\ \mathrm{m_i}\frac{\mathrm{dr_i}}{\mathrm{dt}} = \mathrm{f_i} \tag{1}$$

represents the force on bead I, which are respectively conservative force dissipative force and random force . All DPD beads are under the action of these three forces.[38]

In addition, under certain collision rules, the bead-spring model constructed by DPD omits atomic details to some extent, retaining the main information that characterizes the simulation system. In DPD simulation, a group of atoms or molecules be coarsely grained into a DPD particle. The initial DPD method introduced random and dissipative forces according to the fluctuation dissipation theory. Later, Warren and Española added conservative forces into the DPD force field.[39] The interaction force between the three beads is only valid within the range of cut-off radius under boundary conditions:

$$f_i = \sum_{i\neq j}(F_{ij}^C + F_{ij}^R + F_{ij}^D + F_{ij}^S) \tag{2}$$

$$F_{ij}^C = a_{ij}(1 - r_{ij})\vec{e}_{ij} \tag{3}$$

$$F_{ij}^D = -\gamma\omega^D(r_{ij})(\vec{e}_{ij}\cdot\vec{v}_{ij})\vec{e}_{ij} \tag{4}$$

$$F_{ij}^R = T\sigma\omega^R(r_{ij})\xi_{ij}\vec{e}_{ij} \tag{5}$$

where, α_{ij} is the repulsive amplitude between beads; $r_{ij} = r_i - r_j$, representing the relative coordinates between the two beads; $\vec{e}_{ij} = r_{ij}/|r_{ij}|$, denoting the directional displacement of mass center from bead J to bead I. γ represent the strength coefficient of dissipative force, and the the strength coefficient of the random force is σ. ω^D is the relative friction between different DPD beads, and ω^R is the magnitude of random force between the same beads[40]: $\omega^D(r_{ij})=[\omega^R(r_{ij})]^2.\sigma^2=2\gamma k_B T$, k_B is Boltzmann constant, T is temperature and k is spring constant.

2.2 Model building

In this article, a schematic diagram of the telechelic polymer is shown in Fig. 1. The end groups on telechelic polymer are reactive and can construct polymers with complex topological structure through cross-linking reaction betweenthe end groups. Conditions for the formation of complex topologies is baesd on the formation of chemical bonds by active end groups through cross-linking reactions. So, complex topologies formed by fixed short chain cross-linking were designed and generated in model. This paper examines a variety of complex topologies as shown in Fig. 2. " N" represents the number of AB_8A-type telechelic polymers that constitute the secondary topology polymer, which is defined as the secondary topology in this paper. According to the structural characteristics, these topological structure are divided into "line" and "star" with end groups,"flower", "ring" and "cage" without end groups, and composite structure with both free end groups and closed rings such as "Tadpole".

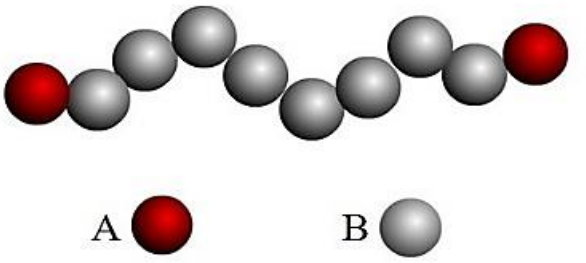

Fig. 1 Schematic diagram of telechelic polymers.

The simulations of 81000 DPD particles at a number density 3 performed in a cube box with a size of 30 × 30 × 30 with periodic boundary conditions. The copolymer volume fraction is 0.1 unless otherwise stated. The interaction parameter αij determined by the characteristic of the beads (either hydrophilic or hydrophobic). We take the interaction parameter between the beads as motion (6).

$$a_{ij} = \begin{pmatrix} & A & B & S \\ A & 25 & \alpha(A,B) & 25 \\ B & \alpha(A,B) & 25 & \alpha(B,S) \\ S & 25 & \alpha(B,S) & 25 \end{pmatrix} \quad (6)$$

The Newton equations for all particles was integrated using Groot-Warren Velocity Verlet (GWVV) algorithm with λ=0.65 γ=4.5, σ=3, dt =0.04, and the integral step length was 5×10^6.The cut-off radius (r_C), bead mass (m) and temperature (k_BT) were allset as 1.0, which were based on previous studies and arguments.[35,41]

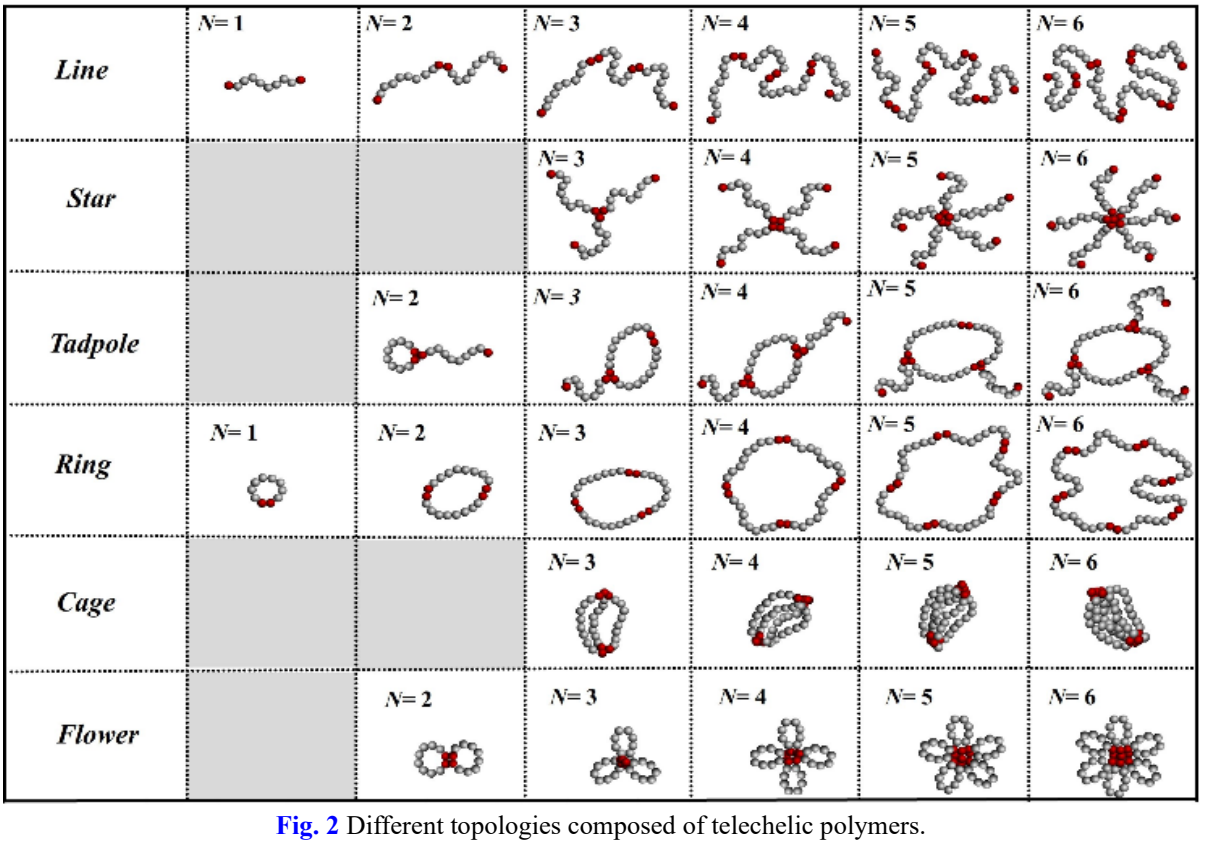

Fig. 2 Different topologies composed of telechelic polymers.

2.3 Results and discussion

We investigated self-assembly micelles with different complex topological structure. Typical micelle aggregates formed by self-assembly of various topological polymers were exhibited in Fig. 3. “Line” and “star” type tended to form cross layer and lamellar micelles, self-assembly of “tadpole” appeared lameller and spherical micelles alternately, “ring” type formed ellipsoid vesicle, “cage” formed vesicles, “flower” type self-assembled to enchased spherical micelles. Furthermore, the effects of solvent conditions, interactions between polymer components, secondary topological structure and chain length of telechelic polymer unit on the assembly aggregates was studied in this paper, and this study analysed the results.

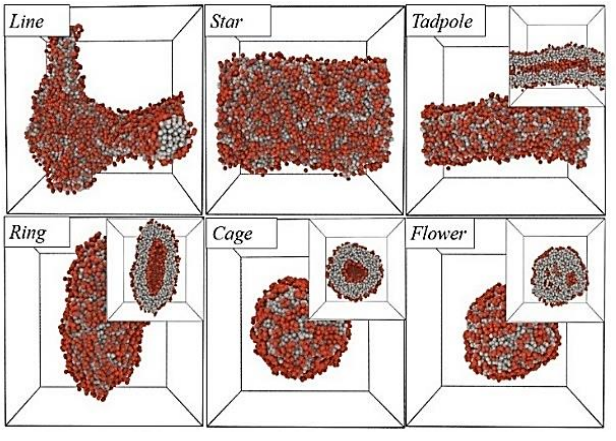

Fig. 3 Snapshoots for self-assembled micelles with diverse topologies in the condition of N=3, α*(B,S)*=50, α*(A,B)*=100.

Fig. 4 shown that the number distribution of the main micelle morphology along the X-axis of hydrophilic block (A) and hydrophobic block (B) in the simulation box. Lamellar and cross laminated micelles were continuous in the box, and the hydrophilic block (A) and hydrophobic block (B) had the same curve trend on the coordinate graph. A series of spheroid micelles, such as vesicles, ellipsoidal vesicles and spherical micelle, only existed in a small part in the simulated box due to their characteristics. The distinguishing characteristic between spherical micelles and vesicles was that the peaks and valleys of the coordinate graph of hydrophilic segment (A) and hydrophobic segment (B) were almost the same. The peak of curve A corresponds to the valley of curve B in vesicles and ellipsoid vesicles. Curve Bhad two (ellipsoid vesicles) or three peaks (vesicles), which was the characteristic of hollow structure reflecting in the coordinate graph.

2.4 Effect of solvent condition on self-assembled structure

In this paper, the end group (A) of the active telechelic polymer was set as hydrophilic block. And the self-assembly behavior of the polymer was driven by the hydrophobic effect of hydrophobic non-reactive block (B). We systematically changed the values of α(*B,S*) to adjust the hydrophobic effect of the polymer, and counted the self-assembly structure distribution of the polymer with various complex topological structure under different solvent conditions (Fig. 5).

The secondary topology (the number of telechelic polymer chains that make up the topology) N was set to 3 as α(*A,B*) is set to 100, five micelle morphologies were observed: cross laminated, lamellar, vesicle, ellipsoidal vesicle and disk micelles. The typical aggregates shown in Fig. 5(b). According to the results, the solvent effect changed the self-assembly structure of the polymer directly. “Line” and “star” self-assembly form cross lamination and lamellar micelle: Under the condition of low block hydrophobicity α(*B,S*)=50-70, the self-assembly micelle is cross; when the hydrophobicity increases α(*B,S*)≥80, standard lamellar micelle appeared. Under the same solvent condition α(*B,S*)=80, we observed that the self-assembled structure changes from lamellar to vesicle with the transition from “line” with end group to “cage” without end group from the perspective of structural changes in topology. The tadpole with end group and loop self-assembled lamellar and vesicle micelle as the similar variation rule as “ring”. It's worth noting that in both “flower” and “cage”, the active end groups form the cross-linked kernel due to the absence of end groups in the polymer topology, causing hydrophobic blocks (B) tend to aggregate to ellipsoidal vesicles with hollow structure. Compared with the flower type, the end groups of the cage was looser, which made the molecular movement of the hydrophobic segment relatively free in the process of self-assembly, and resulting in the appearance of spherical vesicle similar to “ring”. With the

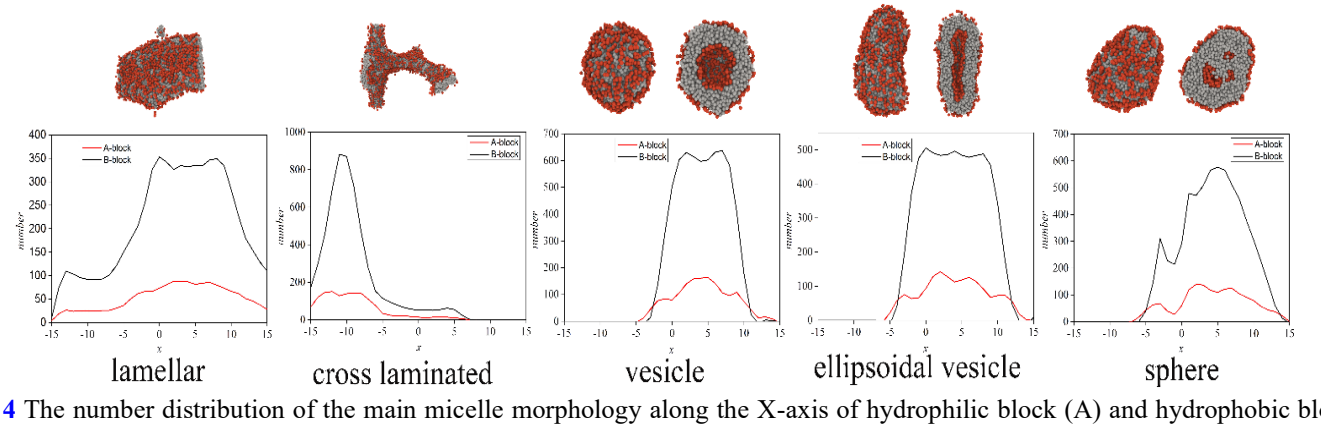

Fig. 4 The number distribution of the main micelle morphology along the X-axis of hydrophilic block (A) and hydrophobic block (B).

increase of α(*B,S*), spherical vesicles transformed into ellipsoid vesicles driven by strong hydrophobic effect. This is because of the compatibility between the hydrophobic blocks (B) and solvent.

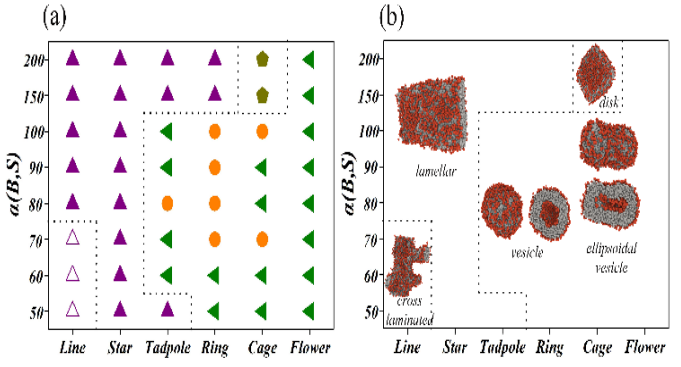

Fig. 5 In the condition of α*(A,B)*=100, N=3: (a) Morphological diagram of micelles formed by diverse topologies in term of interaction parameters α*(B,S)*. (b) Representative morphological snapshots are illustrated for various α*(B,S)* △cross laminated, ▲lamellar,◀ ellipsoidal vesicle, ●vesicle, ⬟disk.

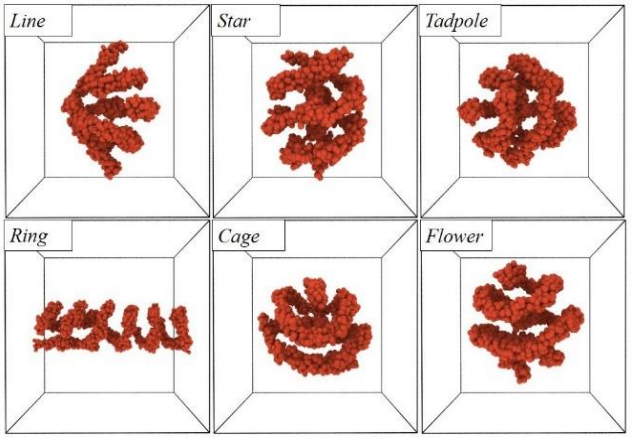

Fig. 6 In the condition of α_{AS}=200, α_{BS}=50, snapshots for self-assembled micelles with diverse topologies.

We also investigated the self-assembly behavior under both hydrophobic condition of α(*A, S*)=200, α(*B,S*)=50. Most self-assembled structures are spherical, and a few are rod micelles surrounded by weak hydrophobic segments (B). The morphology of segment A only can be retained and observed in Fig. 6 a helical structure centered on a small lump of segment A aggregates. "Cage" and "flower" were special compared to other structure consisting of two or three lines forming helical micelles, their self-assembled helical micelles were composed of multiple circles. The self-assembly process shown in Fig. 7, segment A gradually gathered and formed helical structure from scattered distribution at the beginning. The results show that when the end group is hydrophobic, the activity of end group is limited in the process of self-assembly due to the high content of the hydrophilic chain segment. So, the hydrophobic end group continuously forms a helical structure after aggregation, this phenomenon is less affected by the topology. The structure snapshots of flower and linear topology in Fig. 6 can prove it. In addition, the model selects soft interactions where hydrophobic end groups are prone to aggregate continuously to form helical structures.

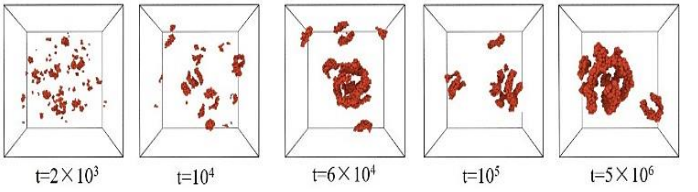

Fig. 7 In the condition of α*(A,S)*=200, α*(B,S)*=50, Sequential snapshots of formation of micelles obtained.

2.5 Effect of polymer component interaction on self-assembled structure

This study investigated the effect of compatibility between the hydrophobic blocks (B) and hydrophilic segment (A) on the self-assembled structure. We regulated the interaction between components by systematically changing the values of α(*A,B*). The morphology of various micelles was shown in Fig. 8, under the conditions of strong hydrophobicity α(*B,S*) =50,100, 200 and secondary topological structure N=3. With the increase of the hydrophobic interaction of the segment B, the micellar structure formed by the telechelic polymer with complex topology becomes more and more complex, and the number of micellar structures increases with the increase of α(*B,S*). When α(*B,S*)=200, Five kinds of self-assembly aggregates observed: lamellar, vesicle, spherical, disk and tube-like micelles. Under strong hydrophobic condition, component interactions had no obvious effect on self-assembly in "line", "star", "tadpole" and "ring" topologies: the major micelle was lamellar. The tube-like micelle of "tadpole" form with α(*A,B*)=60 and vesicle of "ring" form with α(*A,B*) =70. Due to the existence of fixed cross-linked kernel in the structure of cage and flower, the self-assembly structure were obviously affected by component interaction parameters. The cross-linked kernel of "cage" is loose, resulting in the self-assembly structure is intermediate between "ring" and "flower". "Cage" self-assembly formed tube-like, lamellar and vesicle micelles. The "flower" changed from α(*A,B*)=50 to α(*A,B*)=150 as the self-assembly structure changed from ellipsoid vesicle to collapsed red cell structure and then to vesicle with hollow inner ring. The biconcave disk similar to red cell was formed with α(*A,B*) = 60-80.

2.6 Effect of secondary topological structure (N) on self-assembled structure

We investigated the effect of the number N of AB_8A type telechelic polymer composing the secondary topological polymers on self-assembly. Fig. 9 showed the morphology of N=1-6 self-assembly under the condition of α(*A,B*)=100 and α(*B,S*)=50. Five kinds of self-assembly aggregates were observed: cross laminated, lamellar, spherical, vesicle, and ellipsoidal vesicle micelles. "line" self-assembly mainly forms lamellar micelles except for ellipsoidal vesicle at N=1. With the increase of N and the aggregation of hydrophilic block (A), the "star" structure would form lamellar micelles and vesicles

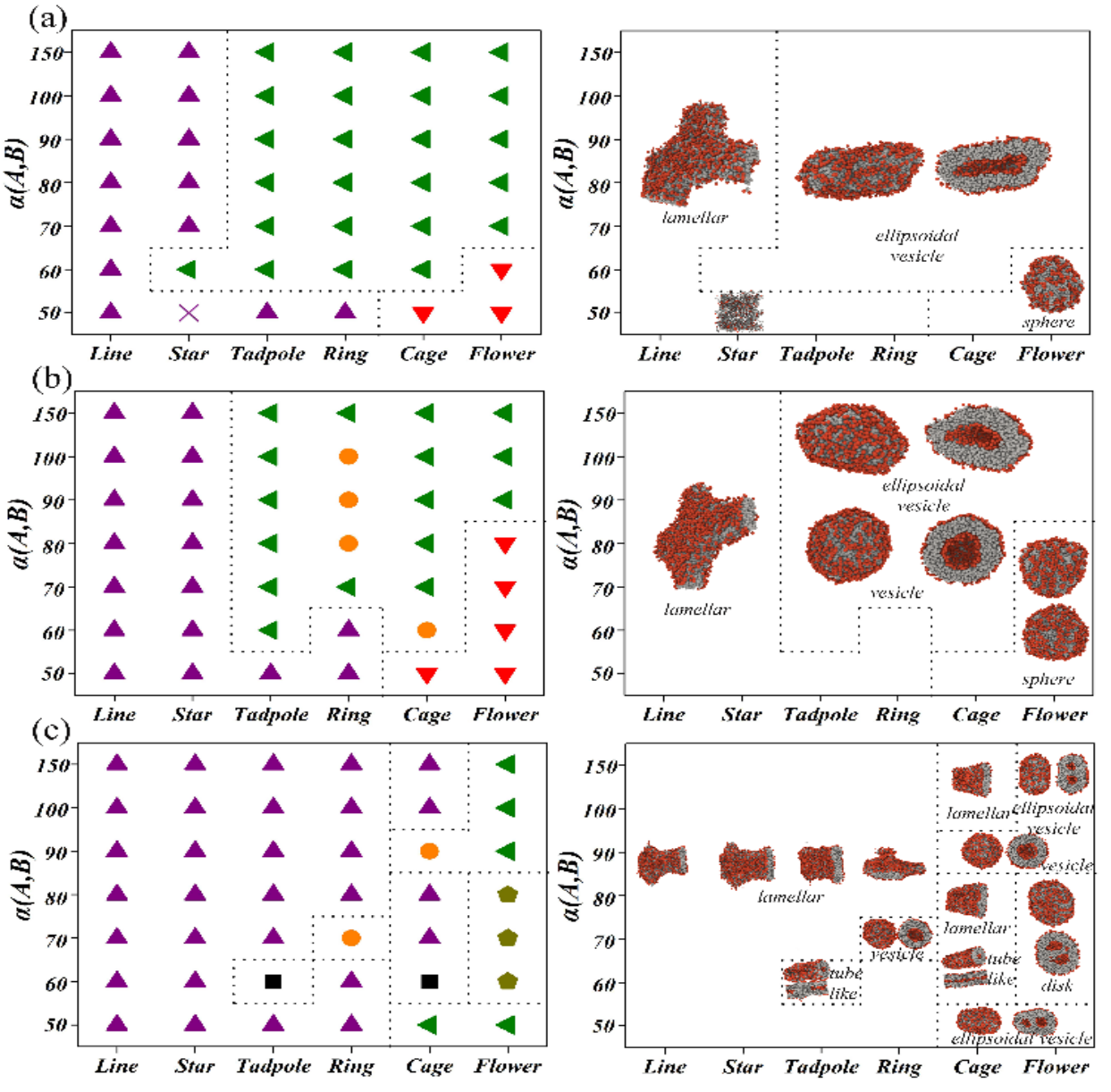

Fig. 8 Morphological diagram of micelles and representative morphological snapshots formed by diverse topologies in term of interaction parameters α*(A,B)* in the condition of α*(B,S)* and N=3. (a) α*(B,S)*=50. (b) α*(B,S)*=100. (c) α*(B,S)*=200. ▲lamellar, ▼sphere, ■tube-like, ●vesicle, ◀ ellipsoidal vesicle, ⬟disk.

respectively: lamellar at N=3,4 and vesicles at N=5,6. "Tadpole" formed vesicles at N=2,6, and the rest of the micelles were lamellar. The micelles of "ring" would change from vesicle to lamellar with the increase of N: the lamellar micelle was above 3, and ellipsoidal vesicle was below 3. Because of the cross-linked kernel aggregated by the hydrophilic segments (A), both "cage" and "flower" tended to form spheroid micelles. "Cage" only formed spherical micelles when N=6, and the others were vesicle micelles. When N=2 and N=3, the "flower shaped" topological structure is self-assembled to form ellipsoidal vesicles. When N>3, the self-assembled structure is spherical micelles, because the formation of vesicle structure is limited by the large content of hydrophilic chain segment (A). In addition, the self-assembly morphology of other topologies also varies significantly with the change of N.

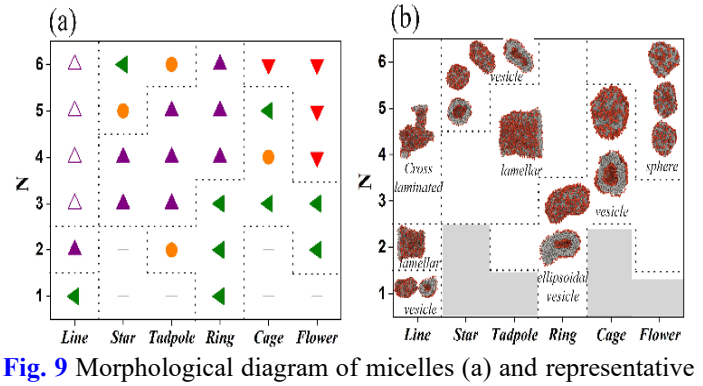

Fig. 9 Morphological diagram of micelles (a) and representative morphological snapshots (b) formed by diverse the number of components of the topology in the condition of α(A,B)=100, α*(B,S)*=50. △cross laminated,▲lamellar, ▼sphere, ◀ ellipsoidal vesicle, ●vesicle.

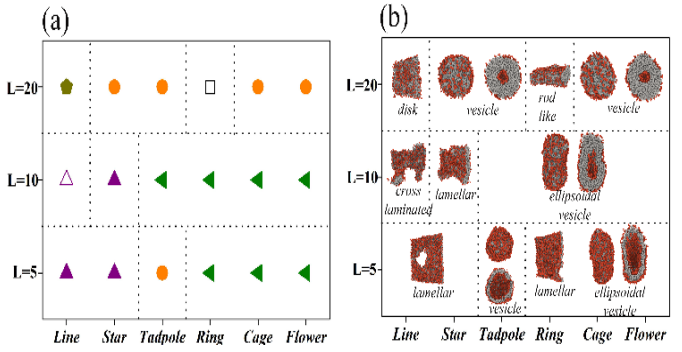

Fig. 10 Morphological diagram of micelles (a) and representative morphological snapshots (b) formed by diverse the chain length of telechelic polymer in the condition of α(*A,B*)=100, α(*B,S*)=60, N=3.△cross laminated,▲lamellar, □rod-like, ◀ ellipsoidal vesicle, ●vesicle.

2.7 Effect of chain length (L) of the telechelic polymer unit on self-assembled structure

Under the condition of α*(A,B*=100, α*(B,S)*=60 and polymer number N=3, we explored the effect of chain length L of telechelic polymer unit on self-assembly structure (Fig. 10). Five kinds of self-assembly aggregates were observed: cross laminated, lamellar, rod-like, ellipsoidal vesicle and vesicle micelles. With the increase of L, the frequency of vesicle micelles will increase, while the lamellar micelles will decrease. It found that shorter hydrophobic chains form vesicles with larger cavities.

2.8 Analysis of formation mechanism of vesicle

We studied the formation mechanism of vesicles and ellipsoid vesicles (Fig. 11). The formation process of vesicles can be observed in Fig. 11 (a): in the initial state, the scattered polymer chains first formed lamellar micelles driven by hydrophobic interactions, then continued to bend toward the center, and finally closed to form vesicle. Figs. 11 (b) and (c) showed the formation process of ellipsoid vesicle: lamellar micelles were formed first, then multiple small vesicles were formed by bending and closing, and then these small vesicles approached spontaneously through Brown motion. When the distance was close enough, the vesicles would contact together on the surface, and finally the internal cavities of small vesicles connected to form the cavity of large ellipsoid vesicle. The mechanisms of vesicle formation are consistent with the results of Wang *et al.* and Jia *et al.*.[42 ,43]

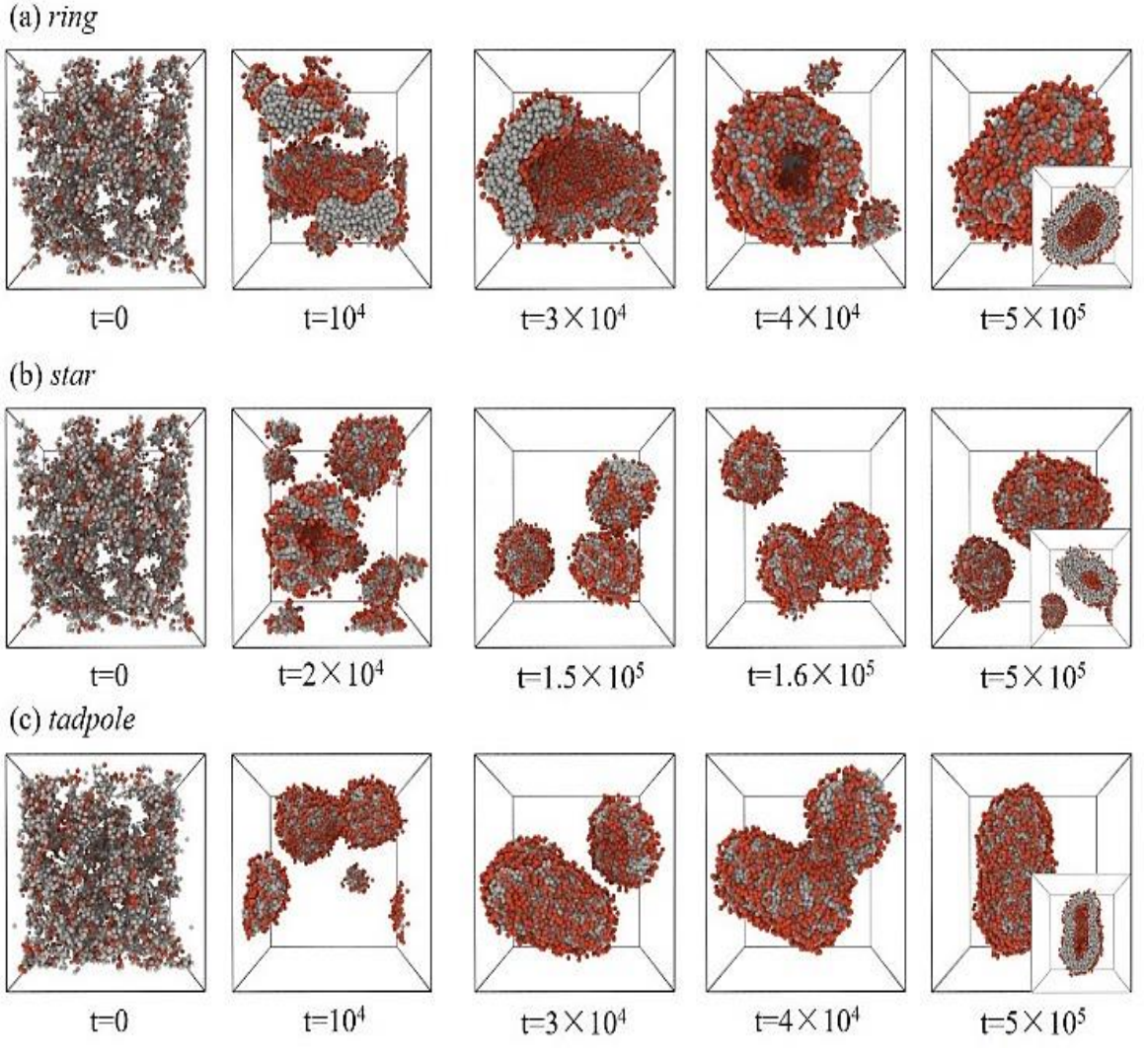

Fig. 11 Sequential snapshots of formation of vesicles and their dominant morphologies obtained from (a) ring, (b)star, (c) tadpole.

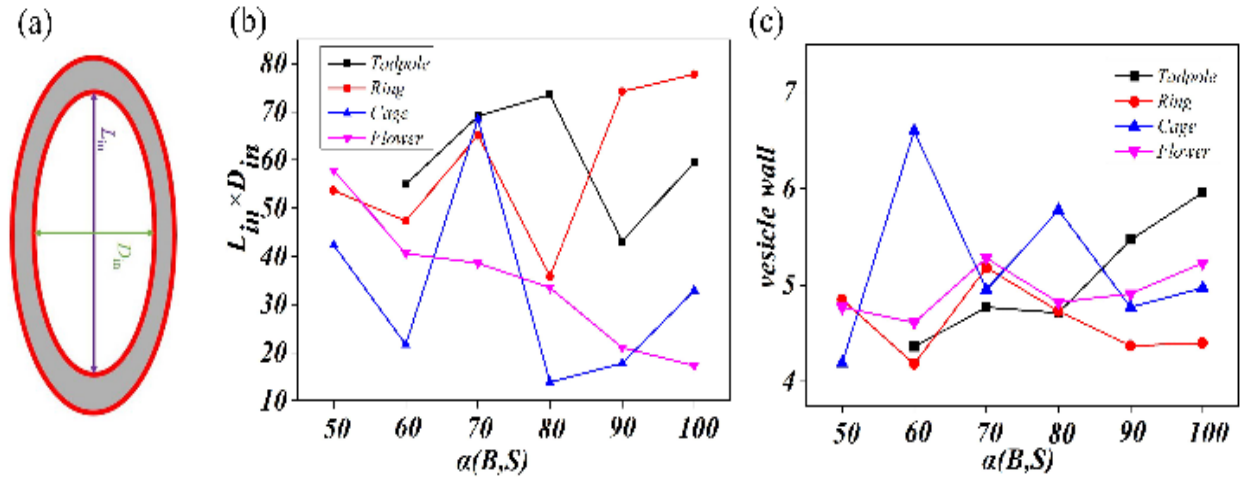

Fig. 12 Structural model and size representation of vesicles. (a) Models of the long axes (Lin) and short axes (Din) of vesicles Structural, (b) Variation curve of Lin×Din with α(*B,S*), (c) Variation curve of the thickness of vesicle wall with α(*B,S*).

At the same time, in order to compare the size of vesicle cavities more intuitively, based on the ellipse area formula: $S=\pi\times L_{in}\times D_{in}/4$, Fig. 12(b) multiplys the $L_{in}\times D_{in}$ values of the major and minor axes of the vesicle. In the condition of α*(A,B)* =100, N=3, Figs. 12(b) and (c) show that self-assembled vesicles with "tadpole" not only have the thinnest vesicle wall, but also have the largest vesicle cavity when α(*B,S*)≤80. However, under the conditions of α(*B,S*)=90 and 100, although vesicles have the thickest vesicle wall, the size of vesicle cavity is still the second largest after the "ring". However, vesicles of the "ring" have the thinnest vesicle wall and the largest vesicle cavity under the conditions of α(*B,S*)= 90 and 100, and also have small vesicle wall and vesicle cavity under the condition of α(*B,S*)≤80. Because of the particularity of "cage" and "flower", small vesicle cavities are common. However, when α(*B,S*)=70, "cage" has the largest vesicle cavity, which is slightly smaller than that of "tadpole".

The ratio *f* of the length of the major and minor axes of the vesicle cavity are listed in Table 1. The *f* of ideal spherical vesicle is 1, and vesicles with *f* < 1.5 are counted as spherical vesicles in our research.

Table 1. In the condition of α*(A,B)*=100, N=3, the ratio *f* of the length of the major and minor axes of the vesicle cavity.

	50	60	70	80	90	100
tadpole		1.93	3.20	1.03	2.09	1.70
ring	4.67	5.23	1.33	1.11	1.13	1.33
cage	5.85	1.88	1.40	2.53	3.34	1.23
flower	3.76	6.00	5.89	3.22	3.28	2.26

3. Conclusion

We studied the self-assembly of telechelic polymers with various complex topologies in dilute solution by using dissipative particle dynamics (DPD). The morphology and the phase diagram of the self-assembly of telechelic polymers were obtained by varying the interaction parameters between solvent and hydrophobic block (B), interactions between polymer components, secondary topological structure and chain length. The results showed that topological structure with loop were more likely to self-assemble into spheroid micelles such as vesicle, ellipsoidal vesicle and disk micelles in weakly selective solvents. However, in highly selective solvents, the self-assembly aggregates of all structure were lamellar except “cage” and “flower” due to the cross-linked kernel forming spherical micelles. Under the condition of hydrophobicity, the segments A with higher hydrophobicity would form continuous double helix structure. The vesicle structure with larger cavitiy were formed by shorter hydrophobic chains, while the vesicle structure formed by long hydrophobic chains were easier to form. Finally, different results been obtained from the mechanism of vesicle formation: the vesicles formed by the bending and closing of lamellar micelles, while the ellipsoid vesicles formed by the contact and fusion of several small vesicles. The simulation result can support for the experiment in theory by predicting the properties of polymer with complex topology structure and provide valuable microscopic insights guiding experimentalists to design functionalized materials by changing the selective of solvent, the chain length and the component of polymers.

The topological structure also affects the size of vesicle cavities and vesicle walls. Vesicles with free-chain topology have thinner vesicle walls and larger vesicle cavities in weakly selective solvents, while in strongly selective solvents the vesicle walls are thickened but still maintain large vesicle cavities. On the contrary, with ring topology, which is cross-linked from the hydrophilic end groups of the polymer chain, has thinner vesicle walls and larger vesicle cavities in the strongly selective solvent, while in the weakly selective solvent, it has thick vesicle walls but still maintains a large vesicle cavity. However, the vesicles of polymers with agglomerated hydrophobic block structure "flower" and "cage" are generally thick vesicle walls and small cavities.

Acknowledgements
This work was supported by Joint fund between Shenyang National Laboratory for Materials Science and State Key Laboratory of Advanced Processing and Recycling of Nonferrous Metals. (18LHPY004; 18LHZD003), National Natural Science Foundation of China (No. 2206060120). Thanks to Zhu Youliang, a researcher from Changchun Institute of Applied Chemistry, Chinese Academy of Sciences, for his technical support in the software GALAMOST.

Conflict of Interest
There is no conflict of interest.

Supporting Information
Not Applicable.

References
[1] Y. Song, T. Xie, R. Jiang, Z. Wang, Y. Yin, B. Li, A.-C. Shi, Effect of chain architecture on self-assembled aggregates from cyclic AB diblock and linear ABA triblock copolymers in solution, *Langmuir*, 2018, **34**, 4013-4023, doi: 10.1021/acs.langmuir.8b00630.
[2] T. Suguri, B. D. Olsen, Topology effects on protein-polymer block copolymer self-assembly, *Polymer Chemistry*, 2019, **10**, 1751-1761, doi: 10.1039/c8py01228h.
[3] M. Schroffenegger, N. S. Leitner, G. Morgese, S. N. Ramakrishna, M. Willinger, E. M. Benetti, E. Reimhult, Polymer topology determines the formation of protein corona on core-shell nanoparticles, *ACS Nano*, 2020, **14**, 12708-12718, doi: 10.1021/acsnano.0c02358.
[4] J.-F. Yin, H. Xiao, P. Xu, J. Yang, Z. Fan, Y. Ke, X. Ouyang, G. X. Liu, T. L. Sun, L. Tang, S. Z. D. Cheng, P. Yin, Polymer topology reinforced synergistic interactions among nanoscale molecular clusters for impact resistance with facile processability and recoverability, *Angewandte Chemie*, 2021, **133**, 22386-22392, doi: 10.1002/ange.202108196.
[5] W. Jiang, Y. Qiang, W. Li, F. Qiu, A.-C. Shi, Effects of chain topology on the self-assembly of AB-type block copolymers, *Macromolecules*, 2018, **51**, 1529-1538, doi: 10.1021/acs.macromol.7b02389.
[6] M. Cao, J.-Q. Wang, P.-C. Chen, J.-T. Xu, Z.-Q. Fan, Cleavage of polystyrene-b-poly(ethylene oxide) block copolymers with a trithiocarbonate linkage in solutions, *Journal of Polymer Science Part A: Polymer Chemistry*, 2010, **48**, 3834-3840, doi: 10.1002/pola.24169.
[7] V. P. Beyer, B. Cattoz, A. Strong, D. J. Phillips, A. Schwarz, C. Remzi Becer, Fast track access to multi-block copolymers via thiol-bromo click reaction of telechelic dibromo polymers, *Polymer Chemistry*, 2019, **10**, 4259-4270, doi: 10.1039/c9py00775j.
[8] J. Ren, X. Hua, T. Zhang, Z. Zhang, Z. Ji, N. Gu, Grafting of telechelic poly(lactic-co-glycolic acid) onto O_2 plasma-treated polypropylene flakes, *Journal of Applied Polymer Science*, 2011, **121**, 210-216, doi: 10.1002/app.33510.
[9] A. S. R. Oliveira, P. V. Mendonça, S. Simões, A. C. Serra, J. F. J. Coelho, Amphiphilic well-defined degradable star block copolymers by combination of ring-opening polymerization and atom transfer radical polymerization: synthesis and application as drug delivery carriers, *Journal of Polymer Science*, 2021, **59**, 211-229, doi: 10.1002/pol.20200802.
[10] S. Li, Z. Ye, Synthesis of narrowly distributed ω-telechelic hyperbranched polyethylenes by efficient end-capping of Pd-diimine-catalyzed ethylene "living" polymerization with styrene derivatives, *Macromolecular Chemistry and Physics*, 2010, **211**, 1917-1924, doi: 10.1002/macp.201000196.
[11] F. Dong, X. Wang, S. Li, J. Hao, X. Tang, R. Kuang, Y. Wang, S. Feng, Applications of α, ω-telechelic polydimethylsiloxane as cross-linkers for preparing high-temperature vulcanized silicone rubber, *Polymers for Advanced Technologies*, 2019, **30**, 932-940, doi: 10.1002/pat.4527.
[12] D. Aoki, G. Aibara, S. Uchida, T. Takata, A rational entry to cyclic polymers via selective cyclization by self-assembly and topology transformation of linear polymers, *Journal of the American Chemical Society*, 2017, **139**, 6791-6794, doi: 10.1021/jacs.7b01151.
[13] E. Barnard, R. Pfukwa, J. Maiz, A. J. Müller, B. Klumperman, Synthesis, structure, and crystallization behavior of amphiphilic heteroarm molecular brushes with crystallizable poly(ethylene oxide) and n-alkyl side chains, *Macromolecules*, 2020, **53**, 1585-1595, doi: 10.1021/acs.macromol.9b02473.
[14] Y. Zhou, L. Li, W. Chen, D. Li, N. Zhou, J. He, P. Ni, Z. Zhang, X. Zhu, A twin-tailed tadpole-shaped amphiphilic copolymer of poly(ethylene glycol) and cyclic poly(ε-caprolactone): synthesis, self-assembly and biomedical applications, *Polymer Chemistry*, 2018, **9**, 4343-4353, doi: 10.1039/c8py00022k.
[15] A. Moreno, A. Jiménez-Alesanco, J. C. Ronda, V. Cádiz, M. Galià, V. Percec, O. Abian, G. Lligadas, Dual biochemically breakable drug carriers from programmed telechelic homopolymers, *Biomacromolecules*, 2020, **21**, 4313-4325, doi: 10.1021/acs.biomac.0c01113.
[16] S. Zhang, M. Arshad, A. Ullah, Drug encapsulation and release behavior of telechelic nanoparticles, *Nanotechnology*, 2015, **26**, 415703, doi: 10.1088/0957-4484/26/41/415703.
[17] M. Kopeć, S. Tas, M. Cirelli, R. van der Pol, I. de Vries, G. J. Vancso, S. de Beer, Fluorescent patterns by selective grafting of a telechelic polymer, *ACS Applied Polymer Materials*, 2019, **1**, 136-140, doi: 10.1021/acsapm.8b00180.
[18] S. Inkinen, G. A. Nobes, A. Södergård, Telechelic poly(L-lactic acid) for dilactide production and prepolymer applications, *Journal of Applied Polymer Science*, 2011, **119**, 2602-2610, doi: 10.1002/app.32763.
[19] C.-C. Wang, Q. -L.Yuan, F. -R. Huang, Preparation of alkynyl terminated telechelic polyimides (API) and properties of T300 carbon fiber cloth/API composites, *Fuhe Cailiao Xuebao/Acta Materiae Compositae Sinica*, 2020, **37**, 519-529, doi: 10.13801/j.cnki.fhclxb.20190523.00
[20] Y. Yu, J. Wang, J. Zong, Synthesis of α, ω-vinyl telechelic polyurethane macromonomer and preparation of polyurethane-

poly(methyl methacrylate) copolymer emulsions via RAFT emulsion polymerization), *Designed Monomers and Polymers*, 2015, **18**, 242-250, doi: 10.1080/15685551.2014.999464.
[21] H. Martinez, M. A. Hillmyer, Carboxy-telechelic polyolefins in cross-linked elastomers, *Macromolecules*, 2014, **47**, 479-485, doi: 10.1021/ma402397b.
[22] Y. Taniguchi, T. Takishita, Y. Kobayashi, N. Arai, T. Kawai, T. Nakashima, Amphiphilic self-assembly of semiconductor nanocrystals with heterogeneous compositions, *EPL (Europhysics Letters)*, 2017, **118**, 68001, doi: 10.1209/0295-5075/118/68001.
[23] A. Iscen, G. C. Schatz, Peptide amphiphile self-assembly, *EPL (Europhysics Letters)*, 2017, **119**, 38002, doi: 10.1209/0295-5075/119/38002.
[24] G. Cocconi, E. Angelis, B. Frohnapfel, M. Baevsky, A. Liberzon, Small scale dynamics of a shearless turbulent/non-turbulent interface in dilute polymer solutions, *Physics of Fluids*, 2017, **29**, 075102, doi: 10.1063/1.4991921.
[25] A. Milchev, A. Nikoubashman, K. Binder, The smectic phase in semiflexible polymer materials: a large scale molecular dynamics study, *Computational Materials Science*, 2019, **166**, 230-239, doi: 10.1016/j.commatsci.2019.04.017.
[26] A. C. Maggs, Multi-scale time-stepping in molecular dynamics, *EPL (Europhysics Letters)*, 2017, **118**, 20006, doi: 10.1209/0295-5075/118/20006.
[27] Y. A. Budkov, A. L. Kolesnikov, N. Georgi, M. G. Kiselev, A flexible polymer chain in a critical solvent: coil or globule? *EPL (Europhysics Letters)*, 2015, **109**, 36005, doi: 10.1209/0295-5075/109/36005.
[28] S. Ma, D. Qi, M. Xiao, R. Wang, Controlling the localization of nanoparticles in assemblies of amphiphilic diblock copolymers, *Soft Matter*, 2014, **10**, 9090-9097, doi: 10.1039/c4sm01446d.
[29] S. Ma, M. Xiao, R. Wang, Formation and structural characteristics of thermosensitive multiblock copolymer vesicles, *Langmuir*, 2013, **29**, 16010-16017, doi: 10.1021/la404157h.
[30] P. Matějíček, M. Uchman, M. Lepšík, M. Srnec, J. Zedník, P. Kozlík, K. Kalíková, Preparation and separation of telechelic carborane-containing poly(ethylene glycol)S, *ChemPlusChem*, 2013, **78**, 528-535, doi: 10.1002/cplu.201300046.
[31] X. G. Qiao, H. J. Wu, Z. Zhou, Q. Q. Tang, X. C. Pang, M. X. Zang, S. Z. Zhou, Simple and facile preparation of lignosulfonate-based composite nanoparticles with tunable morphologies: from sphere to vesicle, *Industrial Crops and Products*, 2019, **135**, 64-71, doi: 10.1016/j.indcrop.2019.04.024.
[32] X. Guo, J. Yang, Preparation of oleic acid-carboxymethylcellulose sodium composite vesicle and its application in encapsulating nicotinamide, *Polymer International*, 2021, **70**, 1604-1611, doi: 10.1002/pi.6256.
[33] Y. Li, F. Xu, X. Li, S.-Y. Chen, L.-Y. Huang, Y.-Y. Bian, J. Wang, Y.-T. Shu, G.-J. Yan, J. Dong, S.-P. Yin, W. Gu, J. Chen, Development of curcumin-loaded composite phospholipid ethosomes for enhanced skin permeability and vesicle stability, *International Journal of Pharmaceutics*, 2021, **592**, 119936, doi: 10.1016/j.ijpharm.2020.119936.
[34] P. J. Hoogerbrugge, J. M. V. A. Koelman, Simulating microscopic hydrodynamic phenomena with dissipative particle dynamics, *Europhysics Letters (EPL)*, 1992, **19**, 155-160, doi: 10.1209/0295-5075/19/3/001.
[35] R. D. Groot, P. B. Warren, Dissipative particle dynamics: bridging the gap between atomistic and mesoscopic simulation, *The Journal of Chemical Physics*, 1997, **107**, 4423-4435, doi: 10.1063/1.474784.
[36] R. K. W. Spencer, P. F. Curry, R. A. Wickham, Nucleation of the BCC phase from disorder in a diblock copolymer melt: testing approximate theories through simulation, *The Journal of Chemical Physics*, 2016, **145**, 144902, doi: 10.1063/1.4964631.
[37] J. Castagna, X. Guo, M. Seaton, A. O'Cais, Towards extreme scale dissipative particle dynamics simulations using multiple GPGPUs, *Computer Physics Communications*, 2020, **251**, 107159, doi: 10.1016/j.cpc.2020.107159.
[38] T. Zhao, X. Wang, L. Jiang, R. G. Larson, Assessment of mesoscopic particle-based methods in microfluidic geometries, *The Journal of Chemical Physics*, 2013, **139**, 084109, doi: 10.1063/1.4819124.
[39] P. Española, P. B. Warren, Perspective: Dissipative particle dynamics, *Journal of Chemical Physics*, 2017, **146**, 150901, doi: 10.1063/1.4979514.
[40] M. Gong, Q. Yu, C. Wang, R. Wang, Simulating surface patterning of nanoparticles by polymers via dissipative particle dynamics method, *Langmuir*, 2019, **35**, 5534-5540, doi: 10.1021/acs.langmuir.9b00066.
[41] X. Liu, C. Zhou, H. Xia, Y. Zhou, W. Jiang, Dissipative particle dynamics simulation on the self-assembly of linear ABC triblock copolymers under rigid spherical confinements, *e-Polymers*, 2017, **17**, 321-331, doi: 10.1515/epoly-2016-0306.
[42] J. Yang, R. Wang, D. Xie, Aqueous self-assembly of amphiphilic cyclic brush block copolymers as asymmetry-tunable building blocks, *Macromolecules*, 2019, **52**, 7042-7051, doi: 10.1021/acs.macromol.9b01393.
[43] J.-L. Bai, D. Liu, R. Wang, Self-assembly of amphiphilic diblock copolymers induced by liquid-liquid phase separation, *Chinese Journal of Polymer Science*, 2021, **39**, 1217-1224, doi: 10.1007/s10118-021-2563-6.